Reviews in Mineralogy & Geochemistry
Vol. 58, pp. 351-374, 2005

Quantitative Constraints on the Rate of Landform Evolution Derived from Low-Temperature Thermochronology

Jean Braun

Research School of Earth Sciences
The Australian National University
Canberra ACT 0200, Australia
(*Now at Géosciences-Rennes, Université de Rennes 1, Rennes 35042, France*)
Jean.Braun@univ-rennes1.fr

INTRODUCTION

In recent years, the nature of the complex interactions between the solid earth and the overlying atmosphere has been the subject of much debate (England and Molnar 1990; Whipple et al. 1999; Braun et al. 1999). Does erosion play an important role in the dynamics of mountain building? Is there a strong feedback into the balance of forces at the crustal scale from mass transport by erosional and depositional processes at the Earth's surface? Or does erosion passively react to changes in the Earth's surface topography to shape mountains with tectonic forces, originating in the underlying convecting mantle, dominating the dynamics of plate interactions and crustal deformation at convergent plate margins?

The answers to these fundamental questions lie in our ability to determine the rate at which surface processes can react to tectonic forcing (Whipple et al. 1999). Where erosion is efficient, the coupling will be strong as the rate of change of surface loading by mass transport will be similar to the rate of creation of topography by crustal deformation. This may lead to a concentration of deformation and thus exhumation in regions of intense erosion (Koons 1990; Willett et al. 1993; Beaumont et al. 2001; Koons et al. 2002, 2003; Braun and Pauselli 2004). Where erosion is relatively inefficient, mountain building is the result of a balance between internal driving forces and those originating from the deflection of an upper free surface; there is no feedback from erosional processes.

Low-temperature thermochronology, such as (U-Th)/He (He) or fission track (FT) dating in apatite and zircon, provides information on the rate at which rocks cool as they are exhumed towards the "cold" Earth surface (Duddy et al. 1988; Warnock et al. 1997; Farley 2000; Reiners and Farley 1999). Because the temperature structure of the uppermost crust, to which the low-temperature systems will be most sensitive[1], is perturbed by the presence of finite amplitude surface topography (Turcotte and Schubert 1982; Stüwe et al. 1994; Mancktelow and Grasemann 1997; Braun 2002b), one can postulate that He and FT dating can be used to provide constraints on the shape of the surface topography in the past and, consequently, on the rate at which it evolved to reach its present-day form (Braun 2002b).

There have been several attempts to extract such information from low-temperature age datasets (Brown et al. 1994; House et al. 1997, 1998; Braun 2002a,b; Ehlers et al. 2003;

[1] The closure temperature of He in apatite is in the range, 55–75 °C, depending on cooling rate and grain size. The annealing temperature range for FT in apatite is in the range 100–120 °C

1529-6466/05/0058-0013$05.00 DOI: 10.2138/rmg.2005.58.13

Reiners et al. 2003b), most of which used the relationship between age and present-day topographic elevation to make inferences on the shape of the landform in the past, typically at the time at which the low-temperature system closed[2]. In this chapter, I will attempt to define how much information is contained in age-elevation datasets that can be used to constrain the rate at which landform evolves on tectonic timescale, the assumptions that are at the core of this interpretation and the methods to extract this information. More importantly, I will try to define a sampling strategy for collecting age-elevation datasets that optimizes the information about the rate of change of topography. I will then succinctly demonstrate how erosion-driven flexural isostasy can affect age-elevation relationships and how thermochronological data can be used to extract information on the strength of the continental lithosphere (i.e., its effective elastic thickness). I will illustrate each of these points with examples based on several thermochronological datasets collected in a range of tectonic and erosional environments.

TOPOGRAPHY AND TEMPERATURE

To illustrate the effect of surface topography on the thermal structure of the underlying crust, let's consider that the shape of the Earth's surface can be approximated by the sum of a finite number of periodic (cosine and sine) functions. In other words, we assume that surface topography can be expanded in an infinite Fourier series:

$$h(x) = \sum_{i=0}^{\infty} h^{c}_{0,i} \cos(2\pi x/\omega) + \sum_{i=0}^{\infty} h^{s}_{0,i} \sin(2\pi x/\omega) \quad (1)$$

Because heat conduction in solids can be approximated as a linear physical process, the total perturbation caused by any topographic surface can be adequately approximated by the sum of the perturbations caused by each of the components of the Fourier series.

The perturbation caused by a periodic topographic function:

$$h^{c}_{i}(x) = h^{c}_{0,i} \cos(2\pi x/\omega) \quad (2)$$

has been shown (Turcotte and Schubert 1982) to be in phase with the topographic signal, directly proportional to the amplitude of the topography, and to decay exponentially with depth at a rate that is proportional to the wavelength of the topographic signal (ω):

$$T(x,z) = h^{c}_{0,i} G_0 e^{-z/\omega} \cos(2\pi x/\omega) \quad (3)$$

where G_0 is the regional vertical temperature gradient. The total perturbation caused by a generic surface topography can therefore be expressed as:

$$T(x,z) = \sum_{i=0}^{\infty} h^{c}_{0,i} G_0 e^{-z/\omega} \cos(2\pi x/\omega) + \sum_{i=0}^{\infty} h^{s}_{0,i} G_0 e^{-z/\omega} \sin(2\pi x/\omega) \quad (4)$$

Note that this relationship is only valid for small amplitude topography (in comparison with

[2] In most of the following discussion, we will assume that each thermochronological system is characterized by a closure temperature, T_c (Dodson 1973), that corresponds to the temperature at which the system "closed," i.e., the temperature at which solid-state diffusion of the daughter product (He) becomes negligible or when fission tracks are retained in the system as annealing becomes negligible. We recognized, however, that the closure of thermochronological systems is a process that takes place over a range of temperature; where accurate estimates of a rock age are determined from a synthetic temperature history, a more sophisticated approach will be used that takes into account the dependence of solid-state diffusion processes on the rate at which the system cools and the size of the diffusing domain (Dodson 1973; Wolf et al. 1996, 1998).

the wavelength) and assumes that the temperature structure is in steady-state. Furthermore, it assumes that conduction is the dominant mechanism at transporting the heat from the Earth's interior towards the upper free surface, advection by tectonic movement and exhumation has been neglected. More complex semi-analytical expressions have been derived that take into account the advection of heat (Stüwe et al. 1994) and provide first-order estimates of the transient solution (Mancktelow and Grasemann 1997), i.e., following the onset or cessation of a tectonic event. An accurate solution of the finite amplitude topography problem, including the effects of a time-varying surface topography can only be obtained by solving numerically the heat transport equation (Braun 2002b).

The approximate solution given by Equation (4) can be used to illustrate the first-order effect of topography on the underlying temperature structure. The conduction of heat acts as a low-pass filter on the topographic signal (Fig. 1): perturbation caused by the short wavelength features of the topography (km scale) is strongly damped and, assuming a "normal" geothermal gradient of 20 °C/km, does not affect the shape of isotherms above a few tens of degree Celsius. At the other end of the spectrum, the long-wavelength features of the topography (10 km scale and larger) affect the temperature structure of the entire crust. Note that in regions of active tectonic exhumation (i.e., where tectonic uplift is compensated by erosion), the geothermal gradient may reach values of up to 100 °C/km or more[3]. In these situations, the perturbation of short wavelength topography can affect higher temperature isotherms.

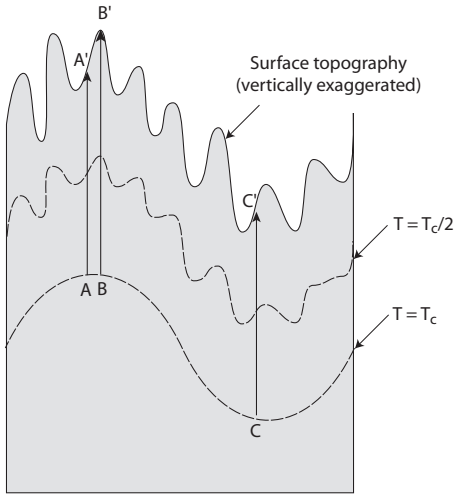

Figure 1. Effect of finite amplitude surface topography on the temperature structure of the underlying crust, using the closure temperature (T_c) of an isotopic dating system for reference. The temperature perturbation decreases exponentially with depth in proportion to the wavelength of the surface topography. Small-scale topographic features do not penetrate sufficiently deep to affect the shape of the closure temperature isotherm, whereas large-scale topographic features causes the closure temperature isotherm to follow the shape of the topography. Small scale relief is ideally suited to extract information about exhumation rate from age-elevation datasets (points A-A' and B-B'), whereas the same data collected across the long-wavelength relief provides constraints on the rate of landform evolution with time (points A-A' and C-C').

This simple, first-order response of a conductive system to perturbation caused by the topography of its upper, cold surface demonstrates that any information that may be contained in age datasets on the past shape of the Earth's surface is limited to a spectral range (a range of wavelengths) that is determined by the local geothermal gradient and the closure temperature of the system. The information is only available for the long wavelength component(s) of the topography, i.e., above a critical wavelength the value of which is determined (to first-order)

[3] The perturbation to the surface geothermal gradient can be shown to be directly proportional to the value of the Peclet number, **Pe** = uL/κ where u is the advection velocity of rocks towards the surface, L the thickness of the layer being exhumed and κ heat diffusivity, characterizing the balance between conductive and advective heat transport in a given tectonic province.

by the ratio of the closure temperature of the dating system and the local geothermal gradient (Braun 2002a):

$$\omega_c = \frac{T_c}{G_0} \tag{5}$$

AGE-ELEVATION DATASETS

Consider an age dataset that has been collected at a range of elevations but in a region characterized by very high topographic relief, or, more exactly, where the wavelength of the topography is short in comparison with the critical wavelength, ω_c. One can then safely postulate that the isotherm corresponding to the closure temperature of the system is not perturbed by the topography (at least locally) and is therefore horizontal. In this situation, depicted by points A-A′ and B-B′ in Figure 1, observed age should be directly proportional to elevation. In fact, one can easily show that the slope of the age-elevation relationship observed along very steep topography is a direct measure of the local mean exhumation rate. Note, that this is true regardless of whether the topography changes with time, as long as the closure temperature isotherm remains "flat" at the scale at which the age sample is collected. Note also that this measure of the local exhumation rate does not rely on an a-priori knowledge of the local geothermal gradient. It is for this reason that age-elevation relationships are commonly collected (e.g., Brown et al. 1994). Unfortunately, in many cases, it is not possible, or simply practical, to sample rocks along a steep topographic feature, either because it does not exist in the area of interest to the investigator, or because it is of very difficult access. One must therefore correct the slope of observed age-elevation relationships for the effect that the topography may have on the shape of the closure temperature isotherm, as suggested by Stüwe et al. (1994). This correction however requires an approximate knowledge of the local geothermal gradient, which is commonly difficult to measure and may lead to inaccurate estimates of the local exhumation rate.

Let's then consider an age dataset collected at a range of elevations but over a very large horizontal distance (points A-A′ and C-C′ in Fig. 1), i.e., much greater than the critical wavelength, ω_c [4]. Assuming that the sampling has been done at a range of wavelengths and that the resulting signal has been properly decomposed into its spectral components, one can easily show that, in the situation where topography does not change through time, observed age values should be independent of elevation. This is a simple consequence of the fact that, at wavelengths much greater than the critical wavelength ω_c, the shape of the closure temperature isotherm follows exactly the shape of the surface topography (Fig. 1). One can then state that any finite variation in age with elevation at a wavelength greater than the critical wavelength ω_c must be related to changes in the shape of the topography at that wavelength. In fact, Braun (2002a) has shown that the ratio of the slope of the age-elevation relationship at long wavelength, normalized by the value of the local exhumation rate (which, in turn, can be obtained from the slope of the age-elevation relationship at short wavelength), is a direct measure of the amount of topographic relief change at the long wavelength over a period of time of the order of the mean value of the age datasets. More importantly, one can easily show that this is the ONLY information contained in an age-elevation dataset on the evolution of the surface topography with time (i.e., with respect to its present-day form).

[4] Care must be taken in collecting such a dataset to avoid aliasing effects that arise when, due to poor sampling, some of the information contained in the relationship between age and elevation is transferred from the short wavelength components of the system to its longer wavelength components.

SPECTRAL ANALYSIS

This dependence of the thermal perturbation of surface topography on the wavelength of the topography and its effect on age-elevation distributions can be formalized by making use of traditional spectral analysis methods. Considering the age, ($a = a_i$, where $i = 1,\ldots,n$ and corresponding elevation, ($h = h_i$, where $i = 1,\ldots,n$) datasets as input and output signals of a dynamic, linear system (equivalent in our case to the process of conductive heat transport in the Earth's crust), one can compute the gain function, $G(\omega_i)$, of the system from the Fourier components of the input and output signals—$F(a)$ and $F(h)$, respectively. Note that the Fourier components and the gain function are complex functions, characterized by a real $R(F)$ and imaginary $I(F)$ parts. Because we know that, to first-order, the thermal perturbation caused by the surface topography is in phase with the surface topographic signal, one can easily show (Braun 2002a) that the imaginary part of the gain function should be nil (or at least much smaller than the real part and can therefore be neglected). The real part of the gain function is given by:

$$R(G) = \frac{C_{12}}{C_{11}}$$
$$C_{12} = R\left[F(a)\right]R\left[F(h)\right] + I\left[F(a)\right]I\left[F(h)\right]$$
$$C_{11} = R\left[F(h)\right]^2 + I\left[F(h)\right]^2$$

Note that the gain function has the dimensions of m.y./km (or s/m in SI units). This relates to our choice of what is the input and the output signal. It may seem more intuitive to use the opposite definition such that the gain function had the dimensions of an exhumation rate or a rate of change of topography with time (km/m.y.). Unfortunately, and as I will show below, in cases where the topography does not change with time, this would lead to infinite values for the gain function at long wavelength, a rather difficult measurement and/or inaccurate calculation to perform.

At short wavelengths, the value of the gain function tends towards the inverse of the mean exhumation rate; at long wavelengths, the value of the gain function tends towards zero if the topography has not changed in the interval of time corresponding to the mean age of the age dataset; it is positive if the topographic relief has increased and it is negative if the topographic relief has decreased. The exact value of the amount of relief change, β, i.e., the ratio of the relief then to the relief now, is given by the following relationship (Braun 2002a):

$$\beta = \frac{1}{1 - G_L / G_S} \tag{6}$$

where G_L and G_S are the asymptotic values of the real part of the gain function at long and short wavelengths, respectively.

These concepts and the spectral method they use can be illustrated if one apply them to a set of "synthetic" age-elevation datasets produced by solving the heat transport equation by conduction (and to a lesser degree by tectonic advection) in a region of the crust that is characterized by finite amplitude topography. The method used is briefly described in the following section and in greater details in Braun (2003). Particles are followed that are exhumed at the surface at a rate of 0.3 km/m.y. Their temperature history is extracted from the solution of the heat transport equation and used to compute the synthetic age-elevation datasets. Three cases are envisaged: one in which topography does not change through time, one in which the topographic relief increases by a factor two over the time span of the "experiment" and one in which the topographic relief decreases by a factor two.

The results, shown in Figure 2, demonstrate that in all three cases, the value of the gain function at short wavelengths always tends asymptotically towards the inverse of the exhumation rate (≈3 m.y./km) while the long wavelength value of the gain function tends towards zero in the case where there is no change in topography, is positive when the topographic relief increases and negative when the topographic relief decreases. Furthermore, estimates of the change in surface relief obtained by applying Equation (6) to each of the three cases (0, 2.5 and 0.55, respectively) are first-order accurate, in comparison to the imposed values (0, 2 and 0.5, respectively).

Note that the definition of what are "long" and "short" wavelengths components of the topographic signal depends on the value of the critical wavelength, ω_c, which is a function of the assumed geothermal gradient and the closure temperature of the dating system used. In the situation considered in the synthetic example (Fig. 2), the critical wavelength is approximately 5 km for apatite-He and 20 km for biotite-Ar. Thus, in an active orogen, characterized by a mean exhumation rate of a few hundreds of meters per million years, apatite-He ages contain information on the rate of relief evolution at wavelengths of 10 km or more; Biotite-Ar ages

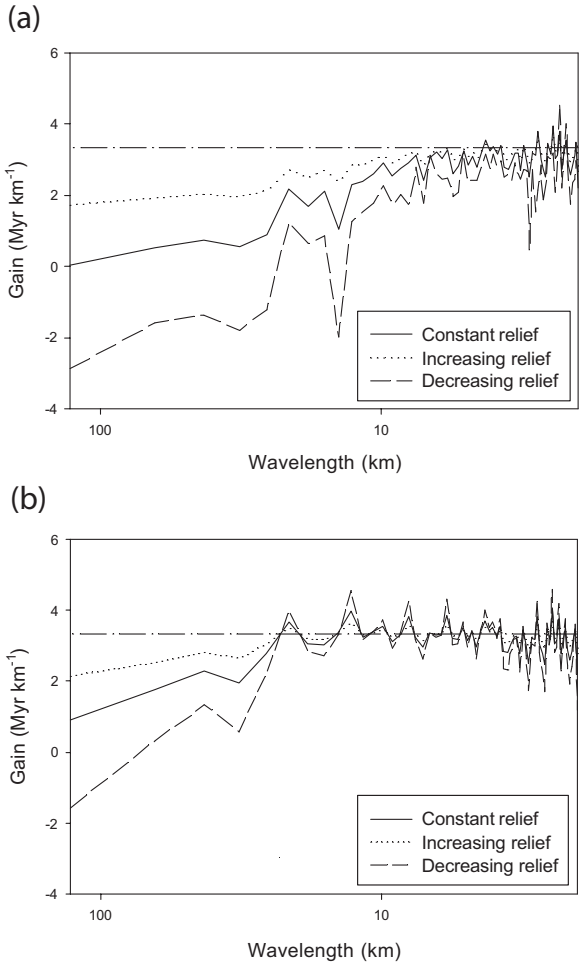

Figure 2. Real part of the gain function between elevation and age from synthetic (a) apatite-He ages and (b) biotite-K/Ar ages computed under the assumption that the surface relief remained constant through time (solid line), increased by a factor of 2 over the last 3 m.y. (dotted line) or decreased by a factor of two over the same time interval (dashed line). The topography has been extracted from GTOPO30 in an area of the Southern Alps, New Zealand, adjacent to Mount Cook. The mixed dashed line represents the gain value corresponding to the inverse of the imposed mean exhumation rate (0.3 km/m.y.). Modified after Braun (2002a).

can only be used to constrain the evolution of the relief at a scale of 20–50 km, which, in most cases, becomes comparable to the scale of the orogen itself. This implies that high-temperature systems (i.e., characterized by a closure temperature greater than 200 °C) can only be used to estimate the rate of change of the orogen-scale topography, in short, the height of the entire mountain belt.

In theory, the spectral method can be used to estimate the value of the gain function at all wavelengths. However, this estimate is accurate only for the spectral components (i.e., the wavelengths) present in the topographic signal. Typically, landforms are dissected by rivers that form valleys. The main trunks of the river system will form valleys that are relatively similar in width and spacing; the tributaries of these main trunks will develop secondary valleys that are more closely spaced and narrower. At the very long wavelength, topography is affected by faulting and differential block uplift which is likely to take place at a wavelength that is determined by the mechanical properties of rocks and the thickness of the layer involved in the deformation (past or present). This implies that accurate measures of the gain function can only be obtained at a small number of critical wavelengths, the value of which is determined by the spectral content of the topographic signal. It is therefore recommended to inspect the power spectrum of the topographic signal and determine which are the "dominant" wavelengths of the topography and focus the spectral analysis, and, optimally, the data collection strategy, at those wavelengths to ensure that the values of the gain function are accurate and meaningful. One can also compute error bars (or confidence intervals) on the gain function estimates by performing the spectral analysis on subsamples of the age-elevation dataset, each half the size of the complete dataset. A statistically significant value for the gain function can be obtained at each wavelength from the mean of the values computed for each of the subsamples and a confidence interval can be extracted from the variance around the mean value (Jenkins and Watts 1968).

Finally, one must note that for the spectral method to be accurate in estimating the mean exhumation rate and the rate of change of surface topographic relief, a specific sampling strategy must be followed, including:

- rocks must be collected along a linear transect at approximately uniform spacing (the exact value of the spacing will depend on the value of the critical wavelength, ω_c; see Braun (2002a) for further details on this);
- rocks must be collected in an area characterized by a uniform exhumation rate, i.e., the transect must be parallel to the strike of the main structures controlling the uplift and related exhumation; this will ensure that the age and elevation signals are stationary, a necessary condition for any Fourier-based spectral method to be accurate;
- horizontal heat advection by movement along low angle structures must be small; one way to avoid this problem is to sample relief produced by large rivers that runs perpendicular to the strike of the main thrust structures and thus parallel to the tectonic transport direction;
- relief must be sampled at all significant wavelengths and at all possible elevations; this may prove rather difficult in many tectonically active areas where local topographic relief may reach several thousands meters.

One can also easily argue that the sampling conditions that are ideal for the use of the spectral method are also those that will yield the most accurate estimate of relief change, i.e., one that does not rely on independent estimates of the local geothermal gradient and/or the mean exhumation rate. In cases where the above sampling guidelines cannot be followed, the spectral method must be abandoned in favor of a less direct, but more flexible approach which we describe in the following section.

Finally, it is worth noting that because it relies on the correlation between elevation and age along a linear transect, the spectral method does not take into account three dimensional effects that might arise from the finite length of valleys and ridges in a direction perpendicular to the transect. In most situations, the thermal perturbation caused by a finite length valley is less significant. This also highlights the need to use a more flexible method to interpret age-elevation datasets in terms of the information they contain on the rate of landform evolution, as proposed in the next section.

3D THERMAL MODELING: PECUBE

Interpreting geological observations to extract meaningful information about the Earth and the dynamic processes that are responsible for its evolution through time is now commonly achieved by using sophisticated numerical models to solve a set of basic differential equations describing the physical processes at play. To interpret thermochronological ages, one needs to predict the temperature history of rocks as they travel through the Earth and are exhumed at the surface. The problem to solve is that of heat transport in a conducting solid where advection by mass transport and production by the decay of radioactive elements may be locally important. The basic partial differential equation to be solved is based on Fourier's law for conductive heat transfer and can be written in the following way (Carslaw and Jaeger 1959):

$$\rho c\left(\frac{\partial T}{\partial t}+\dot{E}\frac{\partial T}{\partial z}\right)=\frac{\partial}{\partial x}k\frac{\partial T}{\partial x}+\frac{\partial}{\partial y}k\frac{\partial T}{\partial y}+\frac{\partial}{\partial z}k\frac{\partial T}{\partial z}+\rho H \qquad (7)$$

where T is temperature, t is time, x, y and z are the spatial coordinates, ρ is density, c is heat capacity, $\dot{E}$ is mean exhumation rate, k is heat conductivity and H is heat production per unit mass. Boundary and initial conditions must also be imposed for this equation to a have a unique, well-defined solution in both space and time. Here we will assume that the base of the crust is held at a constant temperature, T_1, that no heat is lost through the side boundaries and that the temperature at the surface is imposed to follow a typical atmospheric lapse rate γ (i.e., the rate at which the temperature decreases with elevation in the atmosphere):

$$\begin{aligned} T(z=L) &= T_1 \\ \frac{\partial T}{\partial n} &= 0 \quad \textit{on all four vertical sides} \\ T\left[x,y,z=S(x,y,t)\right] &= T_{msl}+\gamma z \end{aligned}$$

The initial temperature distribution is always assumed to correspond to the steady-state solution of the equation ($\partial T/\partial t = 0$).

I have recently developed a numerical method, based on the finite element discretization of space, to solve this equation, including the effect on the heat transfer balance of a time-varying, finite amplitude surface topography. All parameters are imposed, including the rate of exhumation and the geometry of the surface topography at a finite number of times in the past. In between these times, the topography is assumed to change linearly from one configuration to the next. The method is accurate, stable and efficient; it is fully described in Braun (2003) where estimates of its accuracy are also provided. The code is freely available from my web site (*http://rses.anu.edu.au/~jean/PROJECTS/PECUBE/*). The code, named **Pecube**, was used to estimate the synthetic age-elevation datasets used in the previous section to illustrate the accuracy of the spectral method. During the computations, the position and temperature of a set of rock particles that will end up at the surface of the model at the end of the computations are stored. These temperature and depth estimates are used to compute a *P-T-t* (pressure-temperature-time) path for each of the particles which are then used to compute

an age, following the procedure described by Wolf et al. (1998) for (U-Th)/He dating in apatite and by van der Beek et al. (1995) for fission track dating in apatite.

EXAMPLE FROM THE SIERRA NEVADA

One of the most successful attempts to directly measure the "antiquity" of a landform by low-temperature thermochronology was undertaken by House et al. (1998) in the Sierra Nevada of northern California. Two opposing scenarios had been proposed for the evolution of the topographic relief in the area: the first assumes that the present-day relief in the Sierra Nevada was the result of long-term erosion of a landform that was created during the Cretaceous Laramide orogeny (Small and Anderson 1995); the competing scenario assumes that the present-day relief is much younger and resulted from Tertiary surface uplift and dissection, driven by renewed tectonic activity in the area, potentially related to subduction along the nearby plate margin, or to an abrupt climate change some 5 m.y. ago that would have resulted in an amplification of any paleo-relief and an isostatically-driven uplift of the area (England and Molnar 1990).

Interpreting the Sierra Nevada data using the spectral method

Rocks were collected along a linear transect crossing several km deep canyons at an approximately constant elevation of 2000 m. Rocks were dated by apatite-He. The data is shown in Figure 3. This dataset is still the only one to-date that comes close to being suited for the spectral analysis. Unfortunately, it did not sample the relationship between age and elevation at all possible elevations; furthermore it was not collected with uniform spacing between the sites. This will cause the short-wavelength estimates of the gain function to be highly inaccurate. Fortunately a few short transects can be constructed from this dataset and the one published earlier by House et al. (1997) in the same area from which a consistent, and therefore reliable, estimate of the mean exhumation rate can be derived, i.e., 0.04 km/m.y.

To perform the spectral analysis of the age-elevation dataset, both elevation and age values were linearly interpolated to form a 128 long series of equally spaced "data points."

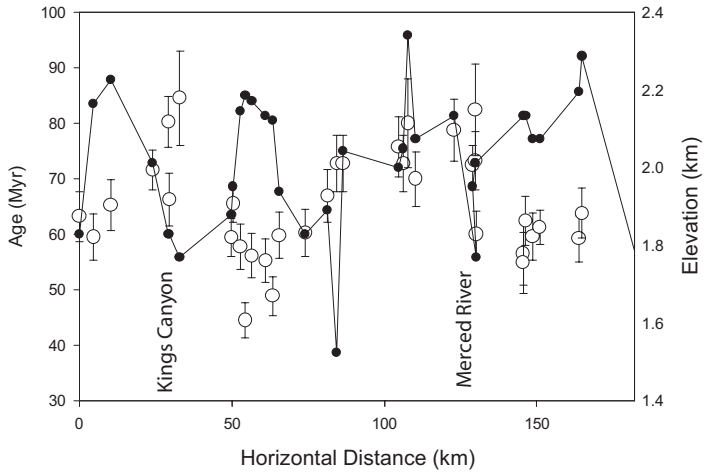

Figure 3. Elevation (open circles) and apatite-He ages (black circles) as a function of distance along a linear transect in the Sierra Nevada, California. See House et al. (1998) for exact location of transect and detailed description of data.

These series were then used to estimate the components of the gain function at wavelengths ranging from 2 to 128 km. The result is shown in Figure 4 and clearly demonstrates that, because the long wavelength estimates of the gain function are negative, the topographic relief at a scale greater than 10–20 km has been decreasing in the last 60–70 m.y. (the mean value of the age data set). Combining the long-wavelength gain estimates with the value of the mean exhumation rate derived from the short transects, leads to the conclusion that the relief amplitude has decreased by a factor of approximately 2. This supports the conclusion at which House et al. (1998) arrived that the large scale topographic features of the area, i.e., the large east-west trending canyons, are indeed the remnants of a much larger amplitude topographic relief that was formed during the Laramide Orogeny. Unlike House et al. (1998), the relief change estimate derived from the spectral analysis is not dependent on any assumption regarding the local past or present geothermal gradient. In fact, that relief has been decreasing for a very long period of time could be concluded from the simple and obvious anti-correlation that exists between age and elevation at the scale of the large valleys (Fig. 3) whereas the strong positive correlation between age and elevation widely documented along several short transects is indicative of the mean exhumation rate of the area driven by the post-orogenic, broad isostatic response to erosional unloading.

Interpreting the Sierra Nevada using Pecube

To illustrate the sensitivity of the relationship between age and elevation for low-temperature systems to landform evolution, we can use **Pecube** to predict the distribution of ages under the two different landform evolution scenarios. I first selected an area around Kings Canyon for which I extracted a 1 km DEM from GTOPO30. Both scenarios have the same initial conditions: it is postulated that the surface relief was twice as large as today's. Numerically I imposed that the surface topography has the same shape as todays' but I doubled its amplitude. In the first scenario, it is assumed that within 20 m.y. of the end of the orogenic event relief has been completely eroded away; in other words the area has been "peneplained." It remains at sea level between 50 and 5 m.y.; finally, over the last 5 m.y. of the experiment the present-day topography is formed by a modern, unspecified process. In the second, simpler

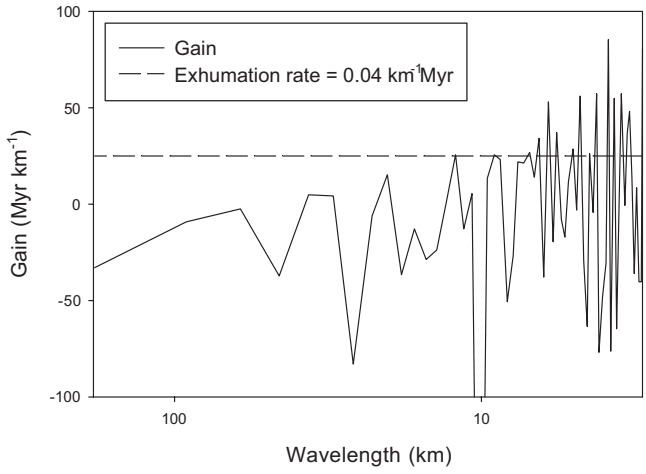

Figure 4. Gain function calculated from the Sierra Nevada data shown in Figure 3. The dashed line corresponds to the gain value equal to the inverse of the exhumation rate calculated from the slope of a well defined age-elevation relationship observed along a very short profile within the area (House et al. 1997). Modified after Braun (2002a).

scenario, relief amplitude decreases linearly from twice its present-day value to todays' value. In both scenarios, I have imposed a mean, slow and steady exhumation rate of 40 m/m.y.

The results of the computations are shown in Figure 5 in terms of predicted age-elevation datasets for each of the two scenarios. In the first scenario, there is a clear linear and positive relation between age and elevation. In the second scenario, there is no apparent correlation between age and elevation. In the first scenario, because there was no surface relief at the time the ages were set, the closure temperature isotherm was perfectly horizontal. That the geometry of the surface topography changed during the late stages of the experiment had no effect on the setting of the ages. Creating the topography simply allowed us to sample the age dataset at various heights. The slope of the age-elevation relationship is exactly equal to the value of the imposed exhumation rate (40 m/m.y.).

In the scenario where the relief decreases linearly over a long period of time, the ages appear to have no correlation to elevation. In fact, two opposite correlations exist at both end of the topographic spectrum: at short wavelengths, there is a positive age-elevation relationship that is proportional to the mean exhumation rate; at long wavelengths, the correlation is negative, reflecting the decrease in topographic relief with time since the rocks passed through their closure temperature. When the entire dataset is plotted in an age-elevation diagram, no clear trend can be extracted. Comparing the results of these two experiments to the distribution of apatite-He ages collected by House et al. (1998) in the Sierra Nevada area (Fig. 5), one is led to conclude that the slow decrease scenario is much more likely than the rapid rejuvenation one (as it predicts a well defined age-elevation relationship at short wavelength only). More importantly, these computations clearly demonstrate how sensitive age datasets are to relief evolution scenarios.

In this and previous sections, we have clearly demonstrated that there is great potential for low-temperature thermochronological datasets to contain important information about landform evolution. Great care must be taken, however, to extract this information from the data and convert it to a meaningful measure of the rate of landform evolution.

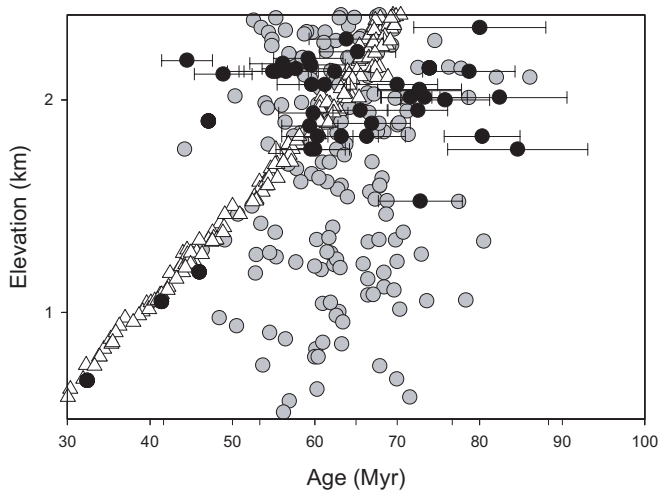

Figure 5. Observed ages (black circles), and predicted ages obtained from the temperature histories computed by **Pecube** assuming that the relief has been decreasing steadily for the last 70 m.y. (grey circles) or that the present-day relief is the product of rejuvenation of the landscape in the last 5 m.y. (white triangle). Modified after Braun (2003).

SLOW EROSIONAL SETTINGS

During the life cycle of an orogenic belt, the post-orogenic phase is commonly accompanied by a slow but steady decrease in surface topographic relief. The processes that act as to decrease the relief (erosion, deposition and transport along the Earth's surface) are still active while the processes that act as to increase the relief (tectonic uplift and/or differential movement on crustal faults) have been turned off. As shown by Kooi and Beaumont (1996), the response of surface processes to an abrupt change in tectonic uplift offers us with an opportunity to estimate the intrinsic rate at which surface processes operate. Most parameterizations of surface processes imply a quasi-linear dependence of erosion and transport rates on local slope (Whipple and Tucker 1999). This, in turn, causes the response of the system to an abrupt cessation in tectonic uplift to be exponential in its time evolution. The e-folding time of this response is regarded as a good measure of the intrinsic rate at which land-forming processes operate in given climatic conditions and for a given set of rock types or lithologies (Kooi and Beaumont 1996).

There are other environments where the geomorphic system is excited by a rapid, quasi-instantaneous event. For example, the rifting between two continents occurring in a region of anomalously high elevation is experienced by both continental fragments as a rapid drop in base level along one of its margins (Gilchrist and Summerfield 1990). The resulting escarpment separating the low-elevation coastal plain from the adjacent continental plateau area has the potential to evolve according to a range of potential scenarios (Gilchrist et al. 1994; Kooi and Beaumont 1994). Some include the retreat of the escarpment as a steep geomorphic feature, others include the slow down-wearing of the escarpment into a gently sloping coastal plain. Because of the absence of tectonic forcing, such environments are thus very useful to isolate the intrinsic response of land-forming processes and have been the target of many attempts to estimate the rate of down-wearing/propagation, both functions of the local rate of stream incision and transport (Gilchrist and Summerfield 1990; Gilchrist et al. 1994; Seidl et al. 1996; Weissel and Seidl 1998; van der Beek et al. 2001, 2002; Brown et al. 2002).

Several studies (Gallagher et al. 1995; Brown et al. 2002; van der Beek et al. 2002; Persano et al. 2002; Braun and van der Beek 2004) have been conducted in recent years to document the rate and nature of escarpment evolution at passive plate margins using thermochronological data collected within the coastal plain at the base of the escarpment. Similarly, several studies have recently focused on constraining the rate of erosional decay of ancient orogenic belts (House et al. 1997, 1998, 2001; Reiners et al. 2003a,b; Braun and Robert 2005).

Isostasy

To state that, in the absence of tectonic forcing, erosional processes can be studied in isolation is, however, an overstatement. Mass transport by erosion and deposition results in unloading/loading of the lithosphere which, in turn, responds by isostatically-driven uplift/subsidence (Turcotte and Schubert 1982). The principle of isostasy states that there is a region within the Earth's interior where, on geological time scales, the strength of rocks is so reduced that no horizontal pressure gradient can be sustained. This region is thought to be located just beneath the lithosphere and is often referred to as the "isostatic compensation depth." The weight of any lithospheric column measured from the compensation depth to the surface must be constant. This is often called the principle of local isostasy and is commonly used to put large-scale constraints on the thickness of the crust and/or the thermal structure of the lithosphere. Furthermore, the lithosphere is characterized by a finite lateral, or flexural, strength (Turcotte 1979) resulting in a damping of the isostatic response to surface loading/unloading for wavelengths that are shorter than the flexural wavelength of the lithosphere. This flexural wavelength can be regarded as the wavelength of deformation of a thin elastic plate subjected to

a point load. The effective elastic thickness of continents (T_e) is a function of their composition (especially crustal thickness) and thermal state and varies typically between 10 and 100 km.

The post-orogenic erosional decay of an orogen and/or the evolution of passive margin escarpment will thus be accompanied by an isostatically-driven rock uplift which may cause an amplification of the erosional processes. For example, assuming local isostasy, the lowering of surface topography by 1 km causes approximately 5 km of isostatic uplift and therefore requires erosion of 6 km of rocks.

Because isostasy controls uplift and, potentially, erosion and exhumation, one must therefore consider the effect that it has on the thermal structure of the lithosphere (this is likely to be small as isostatically driven uplift and exhumation rates are slow) and on the paths of rock particles through that thermal structure. For infinitely small values of the effective elastic plate thickness, the isostatic rebound takes place exactly at the same wavelength as the erosional unloading. In this unlikely situation (the Earth's continental lithosphere always has some finite strength), erosional decay is everywhere amplified by isostatically-driven exhumation. As relief decreases, exhumation is greatest along mountain tops than in valley bottoms and ages are predicted to be anti-correlated to elevation at all wavelengths (T_e = 0 km case in Fig. 6).

For large values of the elastic plate thickness, isostatic rebound is small and uniform across the entire mountain belt. Age is negatively correlated to elevation at long wavelengths, reflecting the decrease in surface topographic relief accompanying the erosional decay of the orogen (Fig. 6); at short wavelengths, a positive relationship exists between age and elevation, the slope of which is proportional to the rate of isostatic rebound experienced by the entire system (T_e = 40 km case in Fig. 6). In this situation, the spectral method should be used as it will provide accurate estimates of both the mean, isostatically-driven erosion rate and the amount of relief change.

At intermediate values of the elastic plate thickness, i.e., similar to the wavelength of the eroding topography, the situation is rather complex and the perturbation from the isostatic rebound on the relationship between age and elevation can be substantial, especially at the

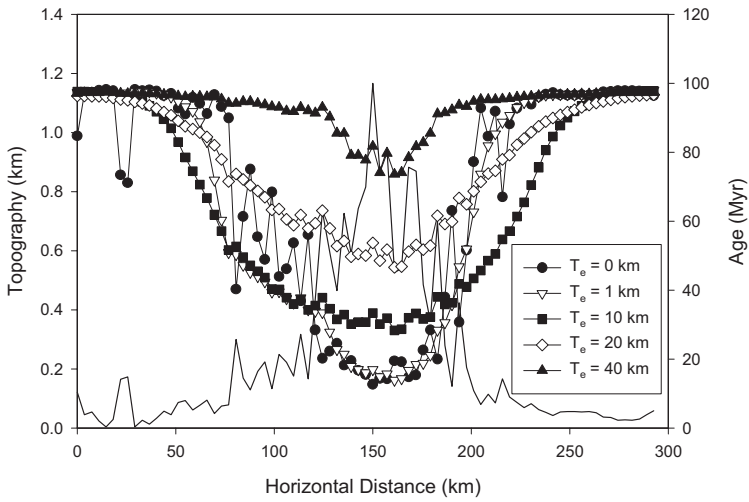

Figure 6. Topography (thin black line) used in **Pecube** to calculate age distributions assuming various values for the effective elastic thickness, Te, for the underlying lithosphere. In all cases it is assumed that relief has decreased steadily by a factor of 4 over the last 100 m.y. Modified after Braun and Robert (2005).

wavelengths that are sensitive to the rate of change of surface relief (T_e = 10 km case in Fig. 6). In this situation, the use of the spectral method is not recommended and a more rigorous, yet computationally costly inversion of the thermochronological data is needed. This is what I propose to describe in the next section and illustrate through a couple of examples.

INVERSION OF AGE-ELEVATION DATASETS

Many existing thermochronological datasets have not been collected with the purpose of using the spectral method to extract from them independent information about the rate of landform evolution. For this reason, they do not fulfill the basic requirements for the method to be accurate: they are not collected along a linear profile perpendicular to the direction of tectonic convergence, they do not sample the relationship between age and elevation at all wavelengths (or at least at the small and long wavelengths contained in the landform) and, most frequently, they do not sample the variation of age across the main geomorphic features of the landscape (the valleys). In fact, for practical reasons, most age datasets are collected along the floor of the main valleys which usually trend in a direction parallel to the tectonic convergence direction and do not sample the main features of the relief, i.e., the relief across the valleys themselves.

For this reason and because the system under investigation may be rendered more complex by the effect of isostasy or horizontal tectonic transport, it is often necessary to perform a more rigorous inversion of the dataset, using for example **Pecube** as a predictor tool. **Pecube** may be regarded as a physically sound method to predict the distribution of ages measured at the Earth's surface for a given erosional scenario and isostatic scenario. The predicted distribution of ages will depend on the imposed erosional scenario, on the assumed degree of flexural compensation of the isostatic response to erosion (through the assumed effective elastic plate thickness), but also on a range of model parameters, including the geothermal gradient, the amount of heat generated in the crust by radioactive decay of K, U and Th, the thermal diffusivity, etc.

One can envisage to run a large number of predictor model runs each corresponding to a different set of model parameters. By comparing the difference between the predicted ages and the observations, one can easily define a degree of "goodness of fit" for each model parameter set. Automated methods have been developed, including the Neighborhood Algorithm (NA) of Sambridge (1999a,b), that efficiently search through parameter space to either map the shape of the misfit function or find the global minimum in misfit which, in turn, should provide the most likely set of model parameters.

However, three situations can arise:

- the misfit cannot be satisfactorily minimized by any combination of parameters; in this case, one or several physical processes that are at play in the natural system have not been incorporated in the predictor model;
- many combinations of the model parameters lead to an acceptable misfit between observations and predictions; no well-defined global minimum can be found; in this case, one can state that the observations do not contain sufficient information to constrain the value of all model parameters; in some cases, only combinations of the model parameters can be constrained;
- the misfit between observations and predictions is clearly minimized for a unique set of model parameters; in this situation, the inversion has led to a clear definition of the "best" or "more likely" model parameters which, in turn, can be translated to determining the contribution/importance of each physical process built into the model.

To illustrate this point and, more generally, the use of inversion methods in interpreting thermochronological datasets to constrain the rate of landform evolution, I will use two examples: one from the Dabie Shan area in eastern China and one from the great coastal escarpment of southeastern Australia. Both examples come from tectonically quiet areas where exhumation (and the subsequent resetting of thermochronological ages) is controlled by the erosional decay of an ancient topography and the associated isostatic uplift.

Post-orogenic erosional decay, example from the Dabie Shan

The Dabie Shan is the result of the collision between the northern edge of the Yangtze craton and the southeastern corner of the Sino-Korean craton that took place during a series of subduction-related episodes of crustal shortening, from the late Paleozoic to the mid-Cretaceous (Schmid et al. 2001). There is debate on whether the orogen was reactivated during the on-going Indo-Asian collision and whether some of the present-day topographic relief is the result of this Cenozoic reactivation (Reiners et al. 2003b). Alternatively, the topography is the erosional remnant of a much larger amplitude relief that was entirely formed in the Cretaceous.

This second hypothesis appears to be supported by apatite (U-Th)/He and FT data recently collected by Reiners et al. (2003b) across the ranges and along a narrow profile near the centre of the orogen (Fig. 7). Today's elevation peaks at approximately 2000 m but most mountain tops do not reach 1500 m (Fig. 7). The thermochronological dataset has been used to constrain the rate evolution of surface relief since the end of the Cretaceous compressional event as well as the effective elastic thickness of the lithosphere, the geothermal gradient and whether the whole area experienced broad-scale (uniform) exhumation during its post-orogenic erosional decay (Braun and Robert 2005). It is the results of this later study that are reported in this section.

Unfortunately, the distribution of the data is such that the spectral method cannot be used to determine the change in surface relief with accuracy. Consequently, we used **Pecube** to solve the 3D heat transport equation and predict the temperature history of rock particles that

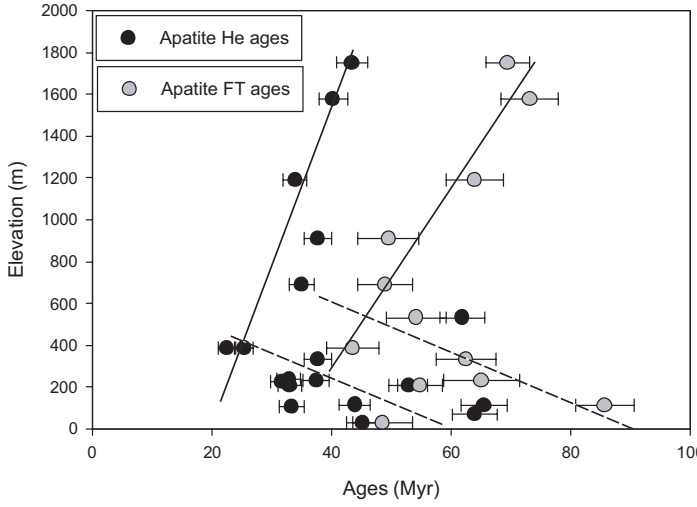

Figure 7. Apatite-He and apatite-FT data collected in the Dabie Shan of eastern China by Reiners et al. (2003). The overall trend is for ages to decrease towards the centre of the orogen (dashed lines); the clear linear trend in age with elevation has been measured along a narrow profile near the centre of the orogen (solid lines). Modified after Braun and Robert (2005).

are exhumed at the surface at the locations where the age data was collected (Braun and Robert 2005). To include the effects of flexural isostasy, we computed the surface load corresponding to each imposed increment in surface topography and computed the incremental thin elastic plate deflection resulting from the application of the load using the two-dimensional spectral method described in Nunn and Aires (1988). We also used a sophisticated inverse method, the Neighborhood Algorithm (NA) (Sambridge 1999a,b) to find the best set of parameters to use in **Pecube** that would predict an age distribution compatible with the observed distribution. NA is used to search through parameter space to map the behavior of a so-called misfit function, that measures the "difference" between the predictions and observations (usually, the L_2 norm of the difference between the observed and predicted age arrays). NA is guided in its mapping by a tessellation of parameter space into Voronoi cells (or neighborhoods) around each point in parameter space representing a forward, **Pecube** model run. NA is designed to find minima in the misfit function and is therefore efficient even for problems involving a large number of parameters.

Result of an NA search are shown in Figure 8. In this case, the Dabie Shan dataset is used as constraints to search in a 6D parameter space, composed of (1) the geothermal gradient (or the temperature at the base of the crust), (2) the timing of the end of the orogenic phase (time at which the erosional decay phase started), (3) the effective elastic thickness of the lithosphere, (4) the amount of relief loss since the end of the orogenic phase, (5) a mean exhumation rate (spatially uniform and constant through time) and (6) the erosional e-folding time scale (the time scale over which half of the original surface relief was eroded away assuming that relief has decreased exponentially with time during the erosional decay phase of the orogen). The results demonstrate that the data does not contain sufficient information to constrain all model parameters, in particular, the basal temperature and erosional e-folding time scale are not constrained at all. The duration of the post-orogenic erosional phase is well constrained at 70 m.y. ago; there appears to be a positive linear relationship between acceptable values for the elastic plate thickness and the amount of relief loss, and a negative linear relationship between acceptable values for the mean exhumation rate and both the effective elastic plate thickness and the amount of relief loss. The predictions of the best fitting model are shown in Figure 9 and corresponds to an elastic plate thickness of ~9 km, a duration of ~70 m.y. for the erosional decay phase, an e-folding time scale for erosion of ~250 m.y., a basal temperature of ~650 °C, a relief loss of ~2.5 and a mean exhumation rate of ~0.02 km/m.y. The fit is very good as the model predictions reproduce not only the orogen-scale trend of ages increasing with decreasing elevation towards the margins of the orogen but also the smaller-scale trend of a strong positive age-elevation relationship along a steep and narrow vertical profile near the centre of the orogen. The results are also consistent with the conclusions reached by Reiners et al. (2003b) using a less sophisticated approach to data inversion. The relatively good fit between observations and model predictions (Fig. 9) demonstrates that the pattern of cooling ages is compatible with a quasi-radially symmetric exhumation caused by erosion-driven isostatic rebound superimposed on a uniform, possibly tectonically-driven, exhumation pattern. This conclusion further illustrate the difficulty to differentiate between the two types of exhumation patterns based on thermochronological data only as already shown by Brandon and Vance (1992) and Brandon et al. (1998).

The information concerning the rate of landform evolution that can be extracted from this dataset is interesting: there has been a decrease in surface relief by a factor of 2 or 3 since the end of the orogenic event some 70 m.y. ago; but whether this relief loss took place very rapidly or has been evolving continuously over the past 70 m.y. cannot be said. The best fitting model suggests that the system has evolved rather slowly, i.e., at a uniform rate. It is also interesting to note that the thermochronological dataset can not only be used to derive constraints on the rate of rock exhumation and amount of relief loss, but also on the effective elastic thickness of

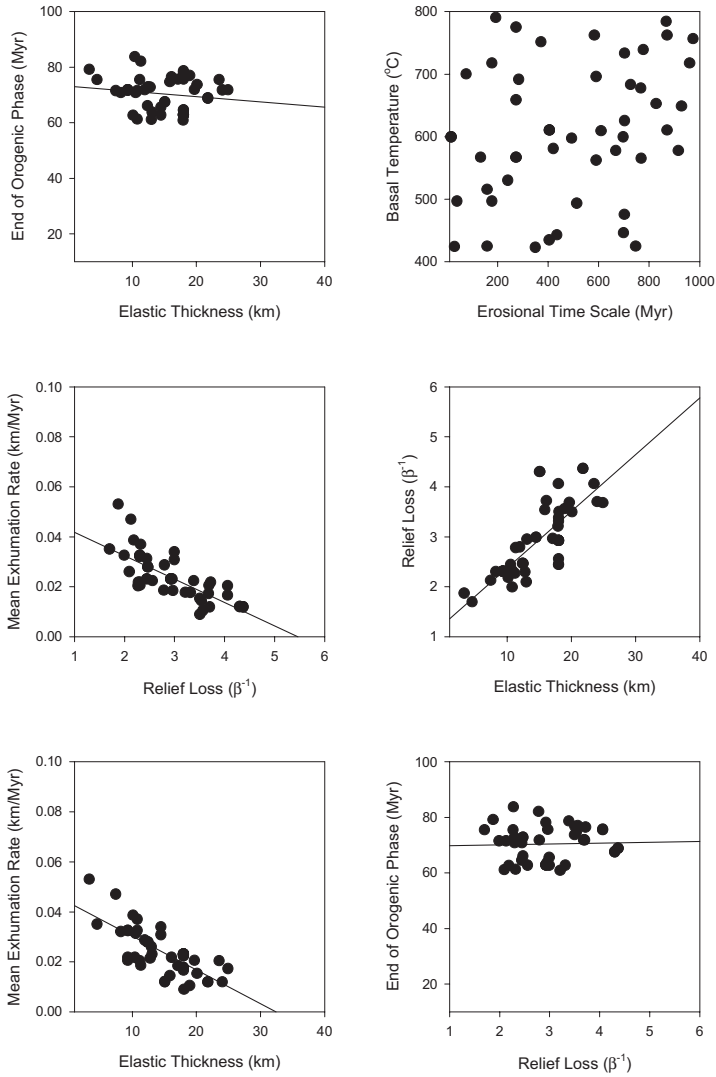

Figure 8. Results of the NA inversion of the Dabie Shan data. Space parameter is of dimension six but results can only be shown by projection onto selected two dimensional sections. Each black dot represent a **Pecube** model run. 17,744 model runs were performed during the search; the 50 best models (i.e., characterized by the lowest misfits) only are shown. Some parameters are well constrained by the data (such as the timing for the end of the orogenic phase); others (such as the basal temperature or the erosional time scale) are not constrained by the data; also shown (black lines) are linear constraints determined by linear regressions between pairs of model parameters (such as elastic thickness and relief loss, or mean exhumation and relief loss). Modified after Braun and Robert (2005).

the lithosphere beneath the area. It is one of the strengths of modern-day inverse methods that they permit to extract from the available data a broader range of constraints on the behavior of the Earth system. They are also very efficient at demonstrating that, sometimes contrary to our intuition, the data does not contain information/constraints on other aspects of the system, in this case, the background geothermal gradient or the erosional e-folding time scale.

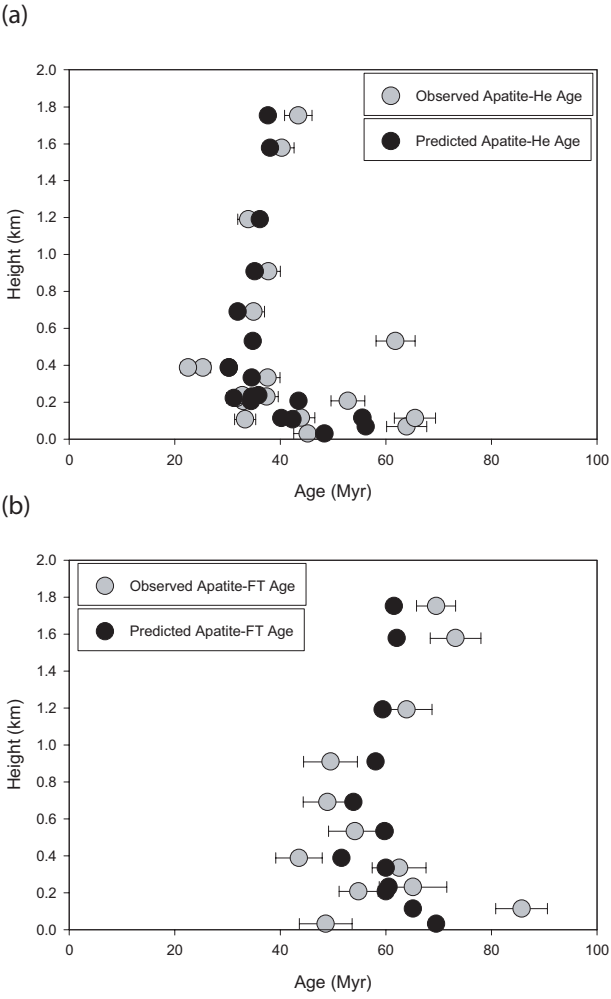

Figure 9. Comparison between the observed ages from the Dabie Shan area Reiner et al. (2003) and the predictions from the **Pecube** run characterized by the smallest misfit. The model predictions reproduce the broad younging of the ages towards the centre of the orogen as well as the well-defined age-elevation relationship along the narrow profile near the centre of the orogen. Modified after Braun and Robert (2005).

The main limitation of the inversion approach/method is its computational requirements. Each of the forward model run performed using **Pecube** took approximately 20 minutes of CPU time on a 2.4 Ghz Pentium IV with very fast access memory. The computations shown in Figure 8 would have taken approximately 246 days to perform if we did not have access to a 128 node cluster of PC's on which the computations took just under 2 days. Clearly, the applicability of this method to invert thermochronological datasets by solving the full 3D heat transfer equation and taking into account the effect of a finite amplitude, time evolving upper surface is limited by the availability of high performance computing facilities. Fortunately, clusters of PC's are now becoming more widely available.

Rate and nature of passive margin escarpment evolution, example from SE Australia

Passive margin escarpments form as a result of continental rifting in an area of anomalously high elevation, such as observed in several continental interiors (Gilchrist and Summerfield 1990). Rifting causes an abrupt drop in base level to which surface processes react. Several hypotheses exist on how escarpments evolve from their original position at the plate margin

to their present-day location some tens to hundreds of kilometers inland. Examples include the escarpment surrounding the southern parts of the African continent (King 1951) and the escarpment flanking the eastern margin of the Australian continent (Ollier 1982).

Two conflicting scenarios for escarpment evolution have received much attention in recent years (Gilchrist et al. 1994; Kooi and Beaumont 1994; Seidl et al. 1996; Weissel and Seidl 1998; van der Beek et al. 2001, 2002; Persano et al. 2002; Braun and van der Beek 2004). One postulates that escarpments retreat landward while keeping their steep morphology, the other postulates that escarpments are rapidly worn down and re-establish themselves at the location of a pre-existing inland drainage divide (Fig. 10). The first "model" for escarpment evolution is called the Escarpment Retreat (ER) model, the alternative model is called the Plateau Down-wearing (PD) model (van der Beek et al. 2001).

Several low-temperature datasets have been collected recently along the coastal plains adjacent to well-defined passive margin escarpments (Morley et al. 1980; Gallagher et al. 1995; Brown et al. 2002; Persano et al. 2002), in an attempt to constrain the nature of the escarpment evolution process and the rate at which it took place. Recently, apatite-He ages have been measured from samples collected along a transect running perpendicular to the escarpment of southeastern Australia, in the coastal plains of the Bega Valley (Persano et al. 2002). The data suggests a rapid evolution of the escarpment close to its present-day position and morphology, soon after rifting and opening of the Tasman Sea (Persano et al. 2002). By inverse modeling, Braun and van der Beek (2004) demonstrated that the data is indeed indicative of a rapid evolution in the mid-Cretaceous but that it cannot be used to differentiate between the two competing scenarios.

In this inversion, NA was used to search through parameter space and **Pecube** was used to relate geomorphic scenarios to predicted thermal histories and age distributions. The data was used to constrain 4 parameters (1) the nature of the process by which the escarpment evolved to its present-day position (i.e., following the ER or PD scenario), (2) the rate of evolution of

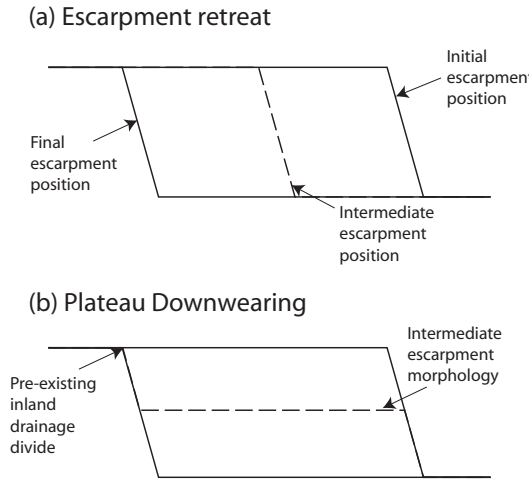

Figure 10. Two scenarios currently proposed for the evolution of a passive margin escarpment. In the escarpment retreat scenario (panel a), the escarpment migrates as a clear topographic step from its initial position near the coast to its present-day position inland; in the plateau down-wearing scenario (panel b), the region comprised between the original escarpment and an pre-existing inland drainage divide is progressively and uniformly eroded away.

the escarpment, (3) the local geothermal gradient, and (4) the effective elastic thickness of the underlying lithosphere. The results show that the best fit to the data was indeed obtained for models characterized by a rapid evolution of the escarpment (i.e., within 15 m.y. of the end of rifting). More interestingly, the inversion also demonstrated that equally acceptable predictions could be made following either of the two scenarios (Fig. 11). The inversion also suggested that the area must be characterized by a very weak lithosphere and/or high geothermal gradient.

Taking the two best fitting model experiments, one for each of the two scenarios and comparing their predictions in terms of the distribution of predicted ages on the natural topography (Fig. 12), one can deduce from the modeling what are the areas where rocks should be collected and dated to provide the best constraints to discriminate between the two scenarios. Consistently, models based on the escarpment retreat scenario predict younger, reset ages near the base of the escarpment. Braun and van der Beek (2004) argue that vertical profiles taken along the face of the escarpment should provide the best constraints on the mode of evolution of the escarpment. As demonstrated earlier, the slope of age-elevation datasets along vertical or near-vertical profiles provides an accurate estimate of the local rate of exhumation. The PD scenario predicts significantly slower local erosion rate than the ER scenario; this difference should be measurable, especially along the face of the escarpment where significant relief exists. Alternatively, a linear transect running parallel to the escarpment and sampling the long-wavelength relief along the face of the escarpment would provide direct estimates of the rate of relief evolution which is markedly different under the two proposed scenarios (Braun and van der Beek 2004).

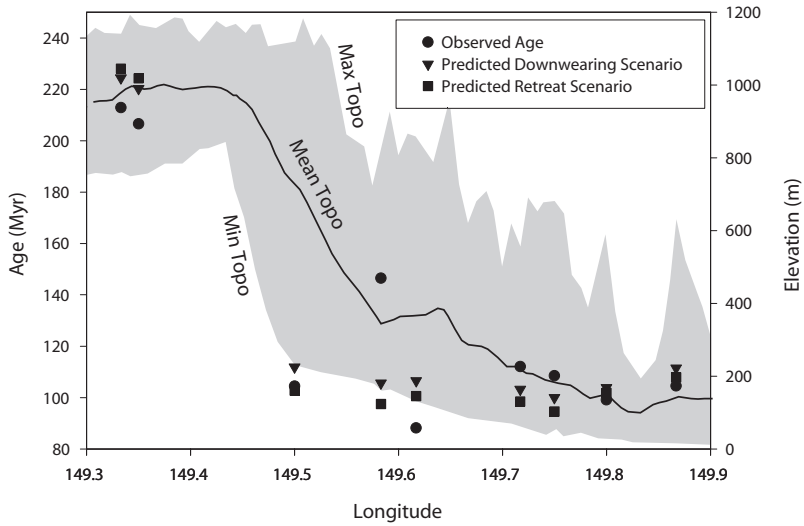

Figure 11. Mean, maximum and minimum elevation in a narrow strip perpendicular to the escarpment in the Bega Valley, where (Persano et al. 2002) collected rocks for apatite-He dating. The observed ages (black circles) are compared to the predictions of two **Pecube** model runs; one model run is based on the escarpment retreat scenario (black squares), the other on the plateau down-wearing scenario (black triangle). That the predictions of the two model runs are equally compatible with the observed ages demonstrates that this thermochronological dataset does not contain information on the mode of evolution of the escarpment in southeastern Australia. The parameters of these two model runs were found by NA search; the search demonstrated that the evolution of the escarpment towards its present-day position took place soon after the opening of the Tasman Sea and that the area must be characterized by a low effective elastic thickness and/or geothermal gradient. Modified after Braun and van der Beek (2004).

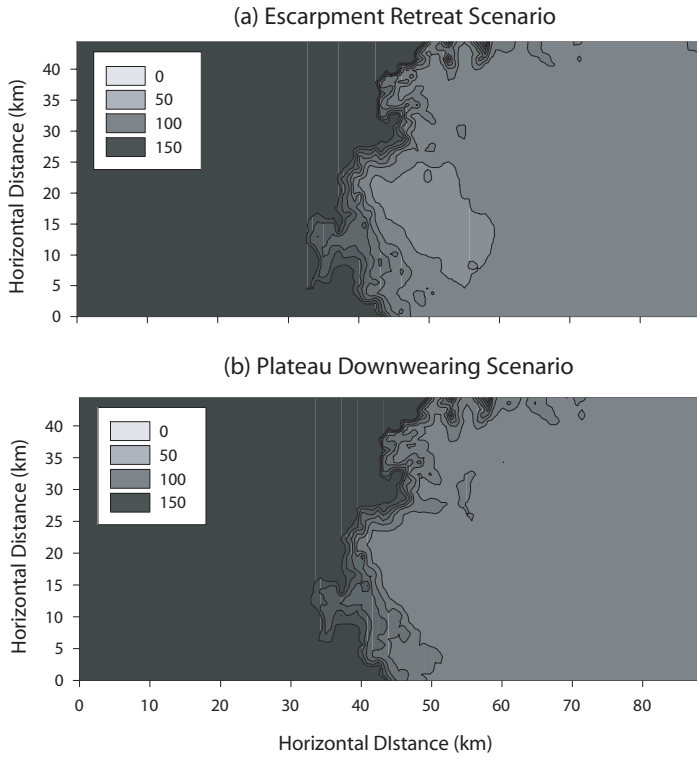

Figure 12. Contour plots of age distributions (in m.y.) predicted from the two "best-fitting" **Pecube** model runs shown in Figure 11. The main difference lies near the bottom of the escarpment. This suggests that this area should be the target of future data collection that could provide the necessary constraints to discriminate between the two hypothesized scenarios. Modified after Braun and van der Beek (2004).

This last point demonstrates how mathematical modeling and the existence of pre-existing data can, and potentially should, be used to define targets for (future) data collection. Mathematical modeling is often regarded as a way to interpret data where, in fact, it should be involved at all stages of investigation, including prior to data collection. In this way, one can make sure that the data collection strategy has been designed to provide optimal constraints on the system being studied. This statement simply reinforces the one made earlier about how to design a sampling strategy that will provide the most useful and independent constraints on the rate of landform evolution through the application of the spectral/gain method. Of course, one cannot avoid the limitations brought to this theoretical consideration by the nature of the geological record: highly spatially variable and incomplete.

CONCLUSIONS AND FUTURE WORK

Recently, much has been learnt about the use and limitations of thermochronological methods in providing constraints on the rate of landform evolution. Sophisticated numerical models have been developed, such as **Pecube**, that have made possible the accurate prediction of the effect of landscape change on the thermal structure of the crust and the distribution of low-temperature age measurements from surface rocks (Braun 2003; Ehlers et al. 2003). It has been clearly demonstrated that the effect is of finite amplitude (i.e., it is much larger than

the uncertainty on age determinations) and strongly variable—it depends on the rate at which landform evolved (Stüwe et al. 1994; Mancktelow and Grasemann 1997; Braun 2002b). In particular, thermochronology has been used to demonstrate the antiquity of some landforms—such as the large-scale relief in the Sierra Nevada (House et al. 1998; Braun 2002a) and/or the Dabie Shan (Reiners et al. 2003b; Braun and Robert 2005). It has also been used to show that some geomorphic features, such as passive margin escarpments, are very dynamic (Persano et al. 2002; Braun and van der Beek 2004): their past history is punctuated by short periods of rapid evolution followed by much longer periods of quiescence.

Much work remains to be done, however, to constrain the potential complex dynamical feedbacks between erosion and tectonics. Much has been said about the potential for erosional processes to focus crustal deformation in regions or high rainfall, thereby linking the evolution of tectonic processes to variations in climate on a local to regional scale (Willett et al. 1993; Beaumont et al. 1999). These ideas remain hypotheses that have been suggested by mathematical models and/or first-order field observations such as the relationship between rainfall and rock exhumation along the western slopes of the Southern Alps of New Zealand (Batt and Braun 1999; Koons et al. 2003), Taiwan (Dadson et al. 2003) or the Himalayan front (Beaumont et al. 2001; Kirby et al. 2003). Much work is still required to understand the complexity of this interaction, including the rate at which landforms can adapt to changing tectonic/uplift conditions (Kooi and Beaumont 1996), how or whether landforms are advected by horizontal tectonic transport (Willett et al. 2001), how the rate of land-forming processes has been affected by the advent of widespread Quaternary glaciations (England and Molnar 1990) or how do these coupled systems behave when subjected to cyclic climatic and therefore erosional conditions as glaciers wax and wane over most of the planet active mountain belts (Braun et al. 1999).

ACKNOWLEDGMENTS

Some of the computations shown in this chapter were performed on the TerraWulf cluster at the Centre for Advanced Data Inference of the Australian National University. The author wishes to thank P. Upton and M. Brandon for useful comments they made on this manuscript.

REFERENCES

Batt GE, Braun J (1999) The tectonic evolution of the Southern Alps, New Zealand: insights from fully thermally coupled dynamical modelling. Geophys J Int 136:403–420

Beaumont C, Jamieson R, Nguyen M, Lee B (2001) Himalayan tectonics explained by extrusion of a low-viscosity crustal channel coupled to focused surface denudation. Nature 414:738–742

Beaumont C, Kooi H, Willett S (1999) Coupled tectonic-surface process models with applications to rifted margins and collisional orogens. In: Geomorphology and Global Tectonics. Summerfield M (ed) John Wiley and Sons Ltd, New York, p 29–55

Brandon M, Roden-Tice M, Garver J (1998) Late Cenozoic exhumation of the Cascadia accretionary wedge in the Olympic Mountains, northwest Washington State. Geol Soc Am Bull 110:985–1009

Brandon M, Vance J (1992) Tectonic evolution of the Cenozoic Olympic subduction complex, Washington State, as deduced from fission track ages for detrital zircon. Am J Sci 292:565—636

Braun J (2002a) Estimating exhumation rate and relief evolution by spectral analysis of age-elevation datasets. Terra Nova 14:210–214

Braun J (2002b) Quantifying the effect of recent relief changes on age-elevation relationships. Earth Planet Sci Lett 200:331–343

Braun J (2003) Pecube: A new finite element code to solve the heat transport equation in three dimensions in the Earth's crust including the effects of a time-varying, finite amplitude surface topography. Comput Geosci 29:787–794

Braun J, Pauselli C (2004) Tectonic evolution of the Lachlan Fold Belt (Southeastern Australia): constraints from coupled numerical models of crustal deformation and surface erosion driven by subduction of the underlying mantle. Phys Earth Planet Int 141:281–301

Braun J, Robert X (2005) Constraints on the rate of post-orogenic erosional decay from thermochronological data: example from the Dabie Shan, China. Earth Surf Proc Land, in press

Braun J, van der Beek P (2004) Evolution of passive margin escarpments: what can we learn from low-temperature thermochronology? J Geophys Res109:F04009, doi:10.1029/2004JF000147

Braun J, Zwartz D, Tomkin J (1999) A new surface processes model combining glacial and fluvial erosion. An Glaciol 28:282–290

Brown R, Summerfield M, Gleadow A (1994) Apatite fission track analysis: its potential for the estimation of denudation rates and implications for models of long-term landscape development. *In:* Process Models and Theoretical Geomorphology. Kirby M (ed) John Wiley and Sons Ltd, New York, p 23–53

Brown R, Summerfield M, Gleadow A (2002) Denudational history along a transect across the Drakensberg Escarpment of southern Africa derived from apatite fission track thermochronology. J Geophys Res 107: 2350, doi:10.1029/2001JB000745

Carslaw H, Jaeger C (1959) Conduction of Heat in Solids. Clarendon, Oxford, third edition

Dadson S, Hovius N, Chen H, Dade W, Hsieh M-L, Willett S, Hu J-C, Horng M-J, Chen M-C, Stark C, Lague D, Lin J-C (2003) Links between erosion, runoff variability and seismicity in the Taiwan orogen. Nature 426:648–651

Dodson MH (1973) Closure temperature in cooling geochronological and petrological systems. Contrib Mineral Petrol 40:259–274

Duddy IR, Green PF, Laslett GM (1988) Thermal annealing of fission tracks in apatite 3. Variable temperature behaviour. Chem Geol 75:25–38

Ehlers T, Willett S, Armstrong P, Chapman D (2003) Exhumation of the central Wasatch Mountains: 2 thermo-kinematic models of exhumation, erosion and low-temperature thermochronometer interpretation. J Geophys Res 108:2173, doi:10.1029/2001JB001723

England P, Molnar P (1990) Surface uplift, uplift of rocks and exhumation of rocks. Geology 18:1173–1177

Farley KA (2000) Helium diffusion from apatite: general behavior as illustrated by Durango fluorapatite. J Geophys Res 105:2903–2914

Gallagher K, Hawkesworth C, Mantovani M (1995) The denudation history of the onshore continental margin of southeastern brazil inferred from fission track data. J Geophys Res 99:18,117–18,145

Gilchrist AR, Kooi H, Beaumont C (1994) Post-Gondwana geomorphic evolution of southeastern Africa: implications for the controls on landscape development from observations and numerical experiments. J Geophys Res 99:12,221–12,228

Gilchrist AR, Summerfield MA (1990) Differential denudation and flexural isostasy in the formation of rifted-margin upwarps. Nature 346:739–742

House M, Wernicke B, Farley K (2001) Paleo-geomorphology of the Sierra Nevada, California, from (U-Th)/He ages in apatite. Am J Sci 301:77–102

House MA, Wernicke BP, Farley KA (1998) Dating topography of the Sierra Nevada, California, using apatite (U-Th)/He ages. Nature 396:66–69

House MA, Wernicke BP, Farley KA, Dumitru TA (1997) Cenozoic thermal evolution of the central Sierra Nevada, California, from (U-Th)/He thermochronometry. Earth Planet Sci Lett 151:167–169

Jenkins GM, Watts DG (1968) Spectral Analysis and its Applications. Holden-Day, Oakland, California, first edition

King LC (1951) South African Scenery. Oliver and Boyd, White Plains, NY

Kirby E, Whipple K, Tang W, Chen Z (2003) Distribution of active rock uplift along the eastern margin of the Tibetan Plateau: inferences from bedrock channel longitudinal profiles. J Geophys Res 108(B4):2217**,** doi:10.1029/2001JB000861

Kooi H, Beaumont C (1994) Escarpment evolution on high-elevation rifted margins: insights derived from a surface processes model that combines diffusion, advection and reaction. J Geophys Res 99:12,191–12,209

Kooi H, Beaumont C (1996) Large-scale geomorphology: classical concepts reconciled and integrated with contemporary ideas via a surface processes model. J Geophys Res 101:3361–3386

Koons P, Norris R, Craw D, Cooper A (2003) Influence of exhumation on the structural evolution of transpressional plate boundaries: an example from the Southern Alps, New Zealand. Geology 31:3–6

Koons P, Zeitler P, Chamberlain C, Craw D, Melzer A (2002) Mechanical links between erosion and metamorphism in Nanga Parbat, Pakistan Himalaya. Am J Sci 302:749–773

Koons PO (1990) Two-sided orogen: collision and erosion from the sandbox to the Southern Alps, New Zealand. Geology 18:679–682

Mancktelow NS, Grasemann B (1997) Time-dependent effects of heat advection and topography on cooling histories during erosion. Earth Planet Sci Lett 270:167–195

Morley ME, Gleadow AJW, Lovering JF (1980) Evolution of the Tasman Rift: Apatite fission track dating evidence from the southeastern Australian continental margin. *In:* Fifth International Gondwana Symposium, pages 289–293, Wellington, New Zealand

Nunn J, Aires J (1988) Gravity anomalies and flexure of the lithosphere at the Middle Amazon Basin, Brazil. J Geophys Res 93:415–428

Ollier CD (1982) The Great Escarpment of eastern Australia: tectonic and geomorphic significance. J Geol Soc Aust 29:13–23

Persano C, Stuart FM, Bishop P, Barford DN (2002) Apatite (U-Th)/He age constraints on the development of the Great Escarpment on the southeastern Australian passive margin. Earth Planet Sci Lett 200:79–90

Reiners P, Ehlers T, Mitchell S, Montgomery D (2003a) Coupled spatial variations in precipitation and long-term erosion rates across the Washington Cascades. Nature 426:645–647

Reiners P, Farley K (1999) Helium diffusion and (U-Th)/He thermochronometry of titanite. Geochim Cosmochim Acta 63:3845–3859

Reiners P, Zhou Z, Ehlers T, Xu C, Brandon M, Donelick R, Nicolescu S (2003b) Post-orogenic evolution of the Dabie Shan, eastern China, from (U-Th)/He and fission-track thermochronology. Am J Sci 303: 489–518

Sambridge M (1999a) Geophysical Inversion with a Neighbourhood Algorithm -I. Searching a parameter space. Geophys J Int 138:479–494

Sambridge M (1999b) Geophysical Inversion with a Neighbourhood Algorithm -II. Appraising the ensemble. Geophys J Int 138:727–746

Schmid R, Ryberg T, Ratschbacher L, Schulze A, Franz L, Oberhansli R, Dong S (2001) Crustal structure of the eastern Dabie Shan interpreted from deep seismic reflection and shallow tomographic data. Tectonophysics 333:347–359

Seidl MA, Weissel JK, Pratson LF (1996) The kinematics and pattern of escarpment retreat across the rifted continental margin of SE Australia. Basin Res 12:301–316

Small E, Anderson R (1995) Geomorphically driven late Cenozoic rock uplift in the Sierra Nevada, California. Science 270:277–280

Stüwe K, White L, Brown R (1994) The influence of eroding topography on steady–state isotherms. Application to fission track analysis. Earth Planet Sci Lett 124:63–74

Turcotte D (1979) Flexure. Adv Geophys 21:51–86

Turcotte DL, Schubert G (1982) Geodynamics: Applications of Continuum Physics to Geological Problems. John Wiley and Sons, New York, first edition

van der Beek P, Andriessen P, Cloetingh S (1995) Morpho-tectonic evolution of rifted continental margins: Inferences from a coupled tectonic-surface processes model and fission-track thermochronology. Tectonics 14:406–421

van der Beek P, Pulford A, Braun J (2001) Cenozoic landscape evolution in the Blue Mountains (SE Australia): Lithological and tectonic controls on rifted margin morphology. J Geol 109:35–56

van der Beek P, Summerfield M, Braun J, Brown R, Fleming A (2002) Modelling post-breakup landscape development and denudational history across the southeast African (Drakensberg Escarpment) margin. J Geophys Res 107(B4):2351, doi:10.1029/2001JB000744

Warnock AC, Zeitler PK, Wolf RA, Bergman SC (1997) An evaluation of low-temperature apatite U-Th/He thermochronometry. Geochim Cosmochim Acta 61:5371–5377

Weissel JK, Seidl MA (1998) Inland propagation of erosional escarpments and river profile evolution across the southeast Australian passive continental margin. *In*: Rivers over Rock: Fluvial Processes in Bedrock Channels. Geophysical Monograph 107. Tinkler KJ, Wohl EE (ed) American Geophysical Union, Washington, p 189–206

Whipple KX, Kirby E, Brocklehurst SH (1999) Geomorphic limits to climate-induced increases in topographic relief. Nature 401:39–43

Whipple KX, Tucker G (1999) Dynamics of the stream-power incision model: implications for height limits of mountain ranges, landscape response timescales and research needs. J Geophys Res 104:17,661–17,674

Willett S, Beaumont C, Fullsack P (1993) Mechanical model for the tectonics of doubly-vergent compressional orogens. Geology 21:371–374

Willett SD, Slingerland R, Hovius N (2001) Uplift, shortening, steady state topography in active mountain belts. Am J Sci 301:455–485

Wolf RA, Farley KA, Kass DM (1998) Modeling of the temperature sensitivity of the apatite (U-Th)/He thermochronometer. Comput Geosci 148:105–114

Wolf RA, Farley KA, Silver LT (1996) Helium diffusion and low-temperature thermochronometry of apatite. Geochim Cosmochim Acta 60:4231–4240